Journal of Experimental Botany, Vol. 70, No. 20 pp. 5853–5864, 2019
doi:10.1093/jxb/erz308 Advance Access Publication June 28, 2019
This paper is available online free of all access charges (see https://academic.oup.com/jxb/pages/openaccess for further details)

RESEARCH PAPER

Phenolics lie at the centre of functional versatility in the responses of two phytochemically diverse tropical trees to canopy thinning

Gerald F. Schneider[1,2,*], Phyllis D. Coley[1,2], Gordon C. Younkin[1], Dale L. Forrister[1], Anthony G. Mills[1] and Thomas A. Kursar[1,2]

[1] Department of Biology, University of Utah, Salt Lake City, UT 84112, USA
[2] Smithsonian Tropical Research Institute, Apartado 0843-03092, Balboa, Ancon, Republic of Panama

* Correspondence: gfschnei@vt.edu

Received 26 September 2018; Editorial decision 21 June 2019; Accepted 23 June 2019

Editor: Nick Smirnoff, University of Exeter, UK

Abstract

Saplings in the shade of the tropical understorey face the challenge of acquiring sufficient carbon for growth as well as defence against intense pest pressure. A minor increase in light availability via canopy thinning may allow for increased investment in chemical defence against pests, but it may also necessitate additional biochemical investment to prevent light-induced oxidative stress. The shifts in secondary metabolite composition that increased sun exposure may precipitate in such tree species present an ideal milieu for evaluating the potential of a single suite of phenolic secondary metabolites to be used in mitigating both abiotic and biotic stressors. To conduct such an evaluation, we exposed saplings of two unrelated species to a range of light environments and compared changes in their foliar secondary metabolome alongside corresponding changes in the abiotic and biotic activity of their secondary metabolite suites. Among the numerous classes of secondary metabolites found in both species, phenolics accounted for the majority of increases in antioxidant and UV-absorbing properties as well as activity against an invertebrate herbivore and a fungal pathogen. Our results support the hypothesis that phenolics contribute to the capacity of plants to resist co-occurring abiotic and biotic stressors in resource-limited conditions.

Keywords: Abiotic stress, biotic stress, chemical defence, light environment, metabolomics, multiple stressors, secondary metabolites, sunflecks, tropical forest, UV radiation.

Introduction

Among the major classes of plant secondary metabolites (SMs), the phenolics have been implicated as the most likely to include compounds with dual abiotic and biotic roles. It is well established that phenolics play an integral part in protecting mesophyll tissue from UV, and it is further hypothesized that phenolics protect against oxidative stress (Jansen *et al.*, 1998; Grace and Logan, 2000; Kolb *et al.*, 2001; Agati and Tattini, 2010; Agati *et al.*, 2013). Likewise, ample demonstration has been given of the anti-pathogen and anti-herbivore roles of many phenolics (Levin, 1971; Bennett and Wallsgrove, 1994; Grayer and Harborne, 1994). However, while strong evidence supports the dual abiotic and biotic functioning of phenolics in general, the extent to which this duality is at play *in planta* within a given plant species remains unclear.

Owing to their habitat and life history, shade-tolerant tropical trees present an ideal ecological context in which to investigate

the potential multifunctionality of phenolics. Growing in the forest understorey as juveniles, such trees are limited by light in their ability to persist, receiving <5% of the photosynthetically active radiation (PAR) reaching the canopy (Chazdon *et al.*, 1996). Here, the survival of these trees is threatened by their restricted capacity to deploy SMs against often abundant herbivores and pathogens (Coley and Barone, 1996). Yet, while even a slight thinning of the forest canopy may significantly increase these trees' capacity to invest in SMs, the increase in PAR is accompanied by additional stressors in the form of higher UVB radiation (Flint and Caldwell, 1998; Jansen *et al.*, 1998) and increased herbivore density (Richards and Coley, 2007; Salgado-Luarte and Gianoli, 2010; Barber and Marquis, 2011). As this transition to higher abiotic and biotic stressor loads is an integral part of the life history of shade-tolerant tropical trees, we may expect selection to have favoured dual-purpose SMs in the phytochemical suites of these species.

Given that the functional properties of phenolics may vary depending on the characteristics of individual phenolic compounds, an evaluation of the functional relationships of a species' entire suite of phenolics across a gradient of stressors requires tracking each individual compound. Such metabolome-scale analysis has recently become feasible thanks to high-throughput mass spectral databases such as the Global Natural Products Social Molecular Networking (GNPS) (Wang *et al.* 2016), which contains >72 000 spectra, as well as mass spectral molecular networking, through which unknown compounds can be classified based on their structural similarity to known compounds (Jansen *et al.*, 2009; Arbona *et al.*, 2013; Wang *et al.*, 2016; Sedio *et al.*, 2017). Using these techniques, we tested the hypothesis that shade-tolerant tropical trees up-regulate phenolic compounds in response to increasingly open light environments as a mechanism of mitigating both abiotic and biotic stressors. Further, we tested the extent to which these phenolics are specialized responses to either abiotic or biotic stressors or are more generalized such that a single compound can have both functions. To do this, we selected two tree species, each producing phenolics of indeterminate function as well as alkaloids and/or terpenoids with specialized anti-pest function, and exposed seedlings to a natural sunfleck regime versus experimentally manipulated PAR approximating the edge of a light gap as well as different levels of UVB. Because herbivores primarily attack expanding leaves (Coley and Barone, 1996), we collected these along with mature leaves. We then evaluated the metabolomic responses and their associations with abiotic and biotic functional properties. To link phytochemical allocation patterns to functional properties, we quantify the UV absorbance, antioxidant power, anti-herbivore activity, and anti-pathogen activity of SM-containing extracts.

Materials and methods

Study species and experimental design

Two shade-tolerant tree species native to lowland forests of central Panama were chosen: *Alseis blackiana* Hemsl. (Rubiaceae) and *Brosimum utile* (Kunth) Pittier (Moraceae). Seeds of *A. blackiana* were collected on Barro Colorado Island, Panama and sown in field-collected soil in June 2013. Seeds of *B. utile* were collected at Parque Nacional San Lorenzo, Panama and sown in a topsoil/sand mixture (described below) in May 2014. Prior to initiation of the experiment, seedlings of both species were grown under shadecloth that transmitted 20% PAR at a shadehouse facility in Gamboa, Panama. In May 2014, 48 individuals of each species were transplanted into pots of 22 cm diameter×40 cm height using a mixture of 30% river sand and 70% topsoil (v/v) collected from a nearby orchard (Dalling *et al.*, 2013). The exterior of each pot was covered with reflective insulation (Reflectix ST24025, Reflectix Inc., Markleville, IN, USA) to prevent heating of the soil and roots in the experimental treatments. Each pot was fertilized initially and every 6 weeks thereafter with 15 ml of Miracle-Gro® fertilizer (24N:8P:16K; micronutrients: B 0.02, Cu 0.07, Fe 0.15, Mn 0.05, Mo 0.0005, Zn 0.06). In June 2014, once all individuals had at least two true leaves, they were randomly assigned to the three treatments. The pots were transported to the experimental shadehouses at dawn and dusk to avoid direct sunlight.

The experiment consisted of three treatments, each incorporating 16 individuals of each species split evenly between two blocks. The names and conditions of the treatments are as follows.

(i) Sunfleck (SF). An *in situ* forest floor treatment was conducted, in which pots were arrayed on top of the leaf litter in an area of forest understorey receiving sunflecks. Pots were positioned 15 m inside the forest edge in two adjoining 2 m×0.5 m rectangles (Supplementary Fig. S1 At *JXB* online). Over the tops of these rectangles was placed a canopy of transparent, UVB-transmitting polyethylene film (0.1 mm thickness, RSHK403-50C-U, Poly-America LP, Grand Prairie, TX, USA), which transmitted 75% of UVB radiation (280–320 nm) and 80% of PAR. The sides of the rectangles were covered with marquisette netting (GardeningWill, Shanghai, China) to exclude herbivorous insects. Each pot was watered by hand every 3 d; the soil surface was always moist to the touch.

(ii) Uniform shade, high UV (USUV+). This was a treatment approximating conditions at the forest floor under a thinned but not open forest canopy (Flint and Caldwell, 1998). This and the following treatment were conducted in shadehouses rather than *in situ* in order to sample leaves that had undergone development entirely under the conditions of the treatments, which the ephemerality of natural canopy openings may have precluded. The shadehouses, two per treatment, consisted of a 3.5 m long×0.7 m wide×0.9 m high PVC frame. The tops and sides, extending down as far as the tops of the pots, were composed of one layer of shadecloth which transmitted 15% of PAR and 15% of UVB, and one layer of the UVB-transmitting polyethylene described in the sunfleck treatment. The remainder of the sides was covered with marquisette netting as in the sunfleck treatment (Supplementary Fig. S1). Slits were cut in the film along the ribs of the PVC frame to provide ventilation, and the centre-top ribs of the frames were lined with three evenly spaced 360° microsprinklers (DIG 8855-5GB, DIG Corp., Vista, CA, USA) which maintained temperature and relative humidity within the mean ±SE of conditions in the shaded perimeter of a nearby treefall gap (Schneider *et al.*, 2019). The sprinklers were run from 10.00 h to 11.30 h and from 13.00 h to 14.30 h daily, and provided sufficient water to keep the soil in the pots moist to the touch.

(iii) Uniform shade, low UV (USUV–). This treatment was identical to USUV+ with the exception of further reduction of UVB transmission. Reduced UVB transmission was achieved by substituting UVB-blocking polyester film for the polyethylene film. The polyester film transmitted 90% of PAR and 10% of UVB (Dura-Lar® 0.13 mm thickness, Grafix, Cleveland, OH, USA).

Temperature and relative humidity were recorded in all treatments using Campbell Scientific CS215 and HMP-50L sensors, with one sensor in the sunfleck treatment and two sensors rotated among the shadehouses of the two uniform shade treatments, coupled with CR800 and CR1000 dataloggers (Campbell Scientific, Logan, UT, USA).

PAR and UVB monitoring

In the sunfleck treatment, PAR sensors (LI-190R, LI-COR Inc., Lincoln, NE, USA) were spaced at 50 cm intervals across the polyethylene film to

monitor light from sunflecks at a fine scale. One sensor was placed above the centre point of each group of four pots, with eight sensors in total. Using a Campbell CR1000 datalogger, mean photosynthetic photon flux density (PPFD) and total PAR were recorded at 5 min intervals for all eight PAR sensors. For the two uniform shade treatments, one PAR sensor was stationed on top of the PVC frame of one of the shadehouses and one PAR sensor was stationed in the centre of the shadehouse, level with the mean height of the plants. Mean PPFD and total PAR were recorded from these sensors at 10 min intervals using a Campbell Scientific CR800 datalogger. PAR was spot-checked across shadehouses of the two uniform shade treatments every 2 weeks using a handheld meter (LI-COR LI-250A) to ensure that logged measurements were representative of all shadehouses. The deviation of spot-checked and logged PAR and the variance across PAR sensors were both <5%. To monitor UVB intensity, we used two Solar Light PMA1106 sensors (Solar Light, Glenside, PA, USA) which recorded at 5 min intervals. In the sunfleck treatment, one sensor was rotated weekly between the PAR measurement locations. The second UVB sensor was rotated weekly among the PAR measurement locations in the uniform shade treatments. The first 18 d of PAR and UVB measurements (31 August–17 September, 2014) were used for statistical comparisons.

Leaf tissue collection and storage

Each pot was inspected weekly to monitor leaf growth, and the first two leaves (or pairs of leaves for *A. blackiana*) for which growth was initiated after the beginning of the experiment were collected simultaneously once the youngest leaf reached ~80% expansion (measured as a percentage of the next oldest fully expanded leaf). This yielded samples of both expanding and mature leaves. Collections were carried out between October and December 2014.

Leaves were excised at the petiole, placed in aluminium foil envelopes, and immediately immersed in liquid nitrogen. The samples were transferred to a –80 °C freezer for storage and then transported on dry ice to the University of Utah where they were kept in a –80 °C freezer to await processing and analysis. As not all 16 individuals of each species per treatment produced two sets of leaves during the experiment, the sample size per treatment, per leaf age, ranged from 5 to 15. All available samples were included in SM extractions and UPLC-MS analyses.

Secondary metabolites: extraction from leaf tissue and fractionation

The frozen leaves were vacuum-dried at –20 °C and ground to a powder as in Wiggins *et al.* (2016). As preliminary analyses indicated that SMs of *A. blackiana* were spread throughout polar and intermediate polarity extract fractions, SM extracts were prepared with aqueous acetonitrile as in Wiggins *et al.* (2016). As preliminary analyses indicated that *B. utile* contained non-polar as well as intermediate polarity SMs, we conducted extractions on this species with a multifraction method described by Endara *et al.* (2015). The fractions containing SMs were then combined for analysis. All extracts were dried and weighed to ±1 mg prior to analysis. The weights provided the gravimetric measurement of extracted metabolites (Fig. 4).

Metabolomic analysis of secondary metabolites

UPLC-MS and tandem MS (MS/MS) were conducted using an I-class Acquity UPLC system with photodiode array UV and Xevo G2 Q-ToF detectors (Waters, Milford, MA, USA). The autosampler temperature was 10 °C and the injection volume was 4 µl. We used an Acquity BEH C18 column (150 mm×2.1 mm ID, 1.7 µm particle size, Waters). The solvents were Optima LC/MS grade water and acetonitrile (Fisher Chemical). Solvent A was water with 0.1% formic acid and solvent B was acetonitrile with 0.1% formic acid. The flow rate was 0.5 ml min^{-1}, and a linear gradient used the following time in minutes/% of solvent B: 0/2%, 2/2%, 4/4%, 22/40%, 32/70%, 35/98%, 36/98%, 40/2%, and 45/2%. UV detection was 210–500 nm with 1.2 nm resolution, five points per second, filter time constant=slow, and exposure time=auto. The mass spectrometer was run in negative, resolution mode using an electrospray ionization (ESI) source with the following parameters: scan time=0.1 s, centroid mode, no collision energy, desolvation gas (N_2) flow rate=600 l h^{-1}, ionization source T=100 °C, capillary voltage= –3.0 kV, sample cone voltage=30 V, extraction cone voltage=4.0 V, desolvation temperature=400 °C. The mass spectrometer was calibrated daily from m/z of 50 to 1200 by direct infusion of 5 mM sodium formate in propanol:water (90:10, v/v). MS data were acquired over a m/z range of 50–2000 Da and corrected using an external reference or lock spray. The lock spray was deprotonated leucine encephalin at m/z 554.2615, 2 ng μl^{-1}, infused at 10 µl min^{-1} with the following parameters: scan time=0.2 s, scan interval=15 s, scans to average=25, mass window= ±0.2 Da, capillary voltage= –2.4 kV.

Mass spectra were collected for all samples prior to and separately from the MS/MS survey runs. We analysed these MS data to find, align, and deconvolute mass spectral peaks using the XCMS and CAMERA packages (Smith *et al.*, 2006; Kuhl *et al.*, 2012) in R statistical software, with analysis parameters as in Endara *et al.* (2015). This allowed us to identify and combine adducts and to exclude in-source fragmentation spectra for our MS/MS analyses.

To collect ion fragmentation spectra via MS/MS, samples were first run in data-dependent acquisition (DDA) mode. Ions that were not fragmented during DDA were targeted for fragmentation in additional runs using an include list (m/z window= ±10 mDa, retention time window=30s). For *A. blackiana*, which has a relatively low number of compounds in its suite of SMs, two samples per treatment were randomly selected for MS/MS. For *B. utile*, which has a more complex suite of SMs, five samples per treatment were randomly selected. The manufacturer's default value was used for the width of the precursor isolation window (LM resolution=4.7). UPLC and MS/MS conditions were the same as in MS mode except for the following: capillary voltage= –2.4 kV, m/z range=30–2000 Da, low mass collision energy ramp 10–30 V, high mass ramp 50–100 V, sample cone voltage 30–40 V; lock spray parameters of scan time=1 s, scan interval=10 s, scans to average=50, mass window= ±0.5 Da. MS/MS acquisition was activated when the intensity of an individual ion exceeded 5000 counts s^{-1}. The maximum number of ions selected for MS/MS from one MS survey scan was five. MS/MS acquisition was discontinued and MS scanning mode reactivated when base peak intensity (BPI) fell below 5000 counts s^{-1} or after 5 s. All m/z included in MS/MS acquisition were subsequently excluded from reacquisition for 10 s. The collision gas was argon (99.999%, Ultra High Purity, Airgas). To ensure that the retention times were correct and the mass accuracy was acceptable, a mixture of standards with a range of retention times and masses was injected at the beginning and end of a set of samples and after every 8–28 samples. Mass accuracy was <6 ppm. Injection of methanol or a blank sample was used to check for artefact or contaminant peaks at the beginning of a set of samples. The standards and blank were also used to condition the column (two injections) prior to collecting data.

Metabolomics data processing

For our *in silico* library, compound names and corresponding SMILES strings of 229 357 compounds from the Universal Natural Products Database of Peking University (Gu *et al.*, 2013) were combined with a library containing an additional 1380 molecules that either have been documented *in planta* or are plausible but theoretical combinatorial variations of these compounds. The resulting file of 230 737 small molecules was parsed into 4615 files of 50 molecules each. Next, the 'predict' module of the program Competitive Fragment Modeling for Metabolite Identification (CFM-ID; Allen *et al.*, 2014) was used to model MS/MS spectra. These computations were performed on the Open Science Grid (Pordes *et al.*, 2007; Sfiligoi *et al.*, 2009; https://www.opensciencegrid.org) in jobs of 50 molecules each using the pre-trained ESI-MS/MS parameters in negative mode provided by Allen (2016).

To conduct molecular networking analyses and library comparisons with our fragmentation data, we combined our *in silico* library with libraries in the GNPS database and ran GNPS networking with the following parameters: minimum matched fragment peaks=6; similarity cosine score for direct match=0.5; similarity cosine score for compound class match=0.3. For constructing molecular networks, the parameters used were: minimum pair cosine score=0.5; minimum matched fragment

ions=6; network TopK=1000; minimum cluster size=2; maximum connected component size=0. After processing via GNPS, molecular networks were uploaded to Cytoscape 3.4.0 (Shannon *et al.*, 2003) for visualization and neighbour-based classification of unknown compounds (Fig. 5). Neighbour-based classification was conducted by examining the library matches of nearest neighbours (separated by one network link) and, if there was a consensus at the structural class level, assigning the unknown compound to the class of its neighbours (Wang *et al.*, 2016; da Silva *et al.*, 2018) (Fig. 5). Unknown compounds with no library matches among their neighbours, or with conflicting matches among their neighbours, were left unclassified. Cytoscape files for visualizing the networks of both species are available in the Dryad Digital Repository (Schneider *et al.*, 2019). Across our two species, the non-phenolic chemical classes represented included phenol-based alkaloids and amines, terpene-containing alkaloids and amines, furanones, and terpenes (Fig. 1). Among phenolics, compounds were grouped based on structural and biosynthetic pathway similarities (Figs 1, 5). The 'flavonoids' group includes flavonoid aglycones and glycosides as well as oligomeric flavonoids such as procyanidins. The 'hydroxycinnamic acids and derivatives' group, or 'HCAs', includes HCA aglycones and glycosides as well as lignin aglycones and glycosides. Finally, the 'other phenolics' group included subclasses that are structurally or biosynthetically distinct from those already mentioned and which accounted for no more than two compounds in any treatment group. This included anthraquinones, benzofuranoids, chalcones, coumarins, miscellaneous 1–2 ring benzenoids, phenylethanoid glycosides, and hydrolysable tannins.

Antioxidant assays

Antioxidant assays were conducted using the FRAP (ferric reducing antioxidant power) assay as described by Benzie and Strain (1999). We used these assays to quantify the total antioxidant power of the SM extract. Assay reactions were carried out in transparent, flat-bottom, polystyrene 96-well plates with 250 µl working volume per well. Aliquots of SM extracts were diluted to 5 mg ml^{-1} for assay reactions, and assayed FRAP values were subsequently multiplied by the dry weight of the SM extract from 0.1 g of dry leaf tissue to calculate the total SM ferric reducing equivalent per unit weight of dry leaf tissue (µM g^{-1}) To ensure that all compounds were assayed in their reduced forms, a reducing agent and buffer were added to the diluted samples 45 min before initiating the assays. The stock reducing solution was composed of 25 mM DTT and 0.12 M NaH_2PO_4, with 1.2 µl of DTT and 16.8 µl of NaH_2PO_4 added

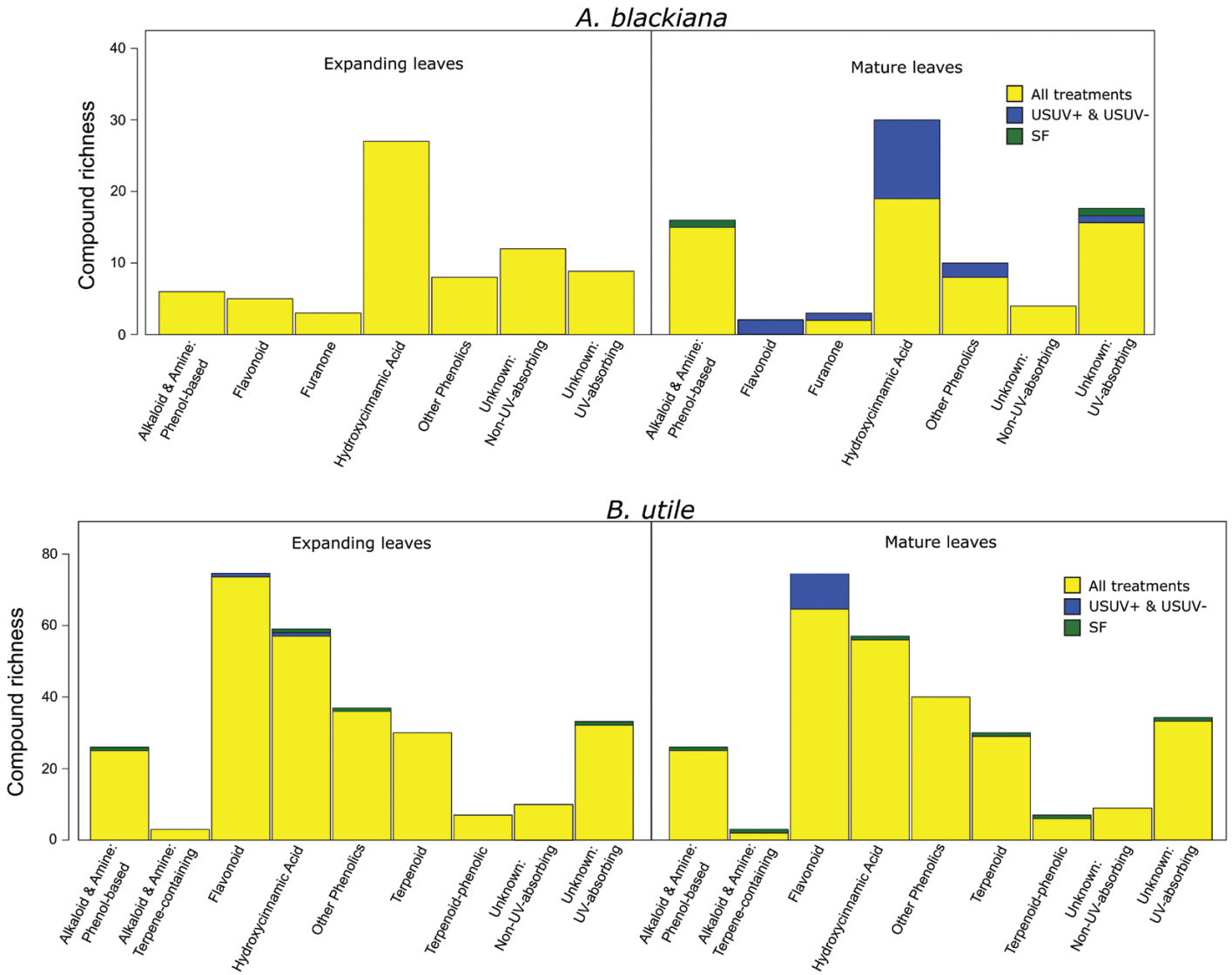

Fig. 1. Richness (total number of compounds) of secondary metabolite classes by species and leaf age. Compounds that were detected in all treatments for a species–leaf age group, which represent the majority of compounds in all cases, are coded as 'all treatments'. Compounds that were only detected in a given treatment are coded as such. The two USUV treatments are grouped together as no compounds were detected in only one of these treatments. (This figure is available in colour at *JXB* online.)

to 12 µl of diluted sample. The reagent mixture was prepared in the ratios described by Benzie and Strain (1999). The standards used for FRAP were 0.5, 1.0, and 2.0 mM Fe(II) supplied by $FeSO4{\cdot}7H_2O$. Assays were initiated by adding 220 µl of reagent mixture to each well with a multichannel pipette and immediately loading plates into a Synergy H1 plate reader (Biotek Instruments Inc., Winooski, VT, USA) with internal temperature set to 37 °C, 540 nm, and a read interval of 16 s.

Fungal pathogen collection and curation

The fungus used in our bioassay was collected from a chlorotic lesion on a leaf of an unidentified Marantaceae species (Supplementary Fig. S2) at Parque Nacional San Lorenzo, Panama. We selected a fungal host plant unrelated to *A. blackiana* or *B. utile* in order to target a fungus that did not specialize on either focal species. Using Koch's postulates (summarized in Agrios, 2005), we isolated the pathogenic strain, used it to reinfect both *A. blackiana* and *B. utile*, and subsequently reisolated the same strain. We also verified its pathogenicity on both study species. Upon isolation, the internal transcribed spacer (ITS) locus of this strain was sequenced at the Smithsonian Tropical Research Institute's Naos Island Laboratories using a 3500 XL DNA analyser (Applied Biosystems, Inc., Foster City, CA, USA). Using primers ITS4 and ITS5, we obtained a sequence of 1041 bp. After transportation of hyphal tissue stored in agar slants to the laboratory of Professor A. Elizabeth Arnold (University of Arizona, Tucson, AZ, USA), the isolate was cultured for use in bioassays. The culture propagated at the University of Arizona was confirmed as the original isolate by re-sequencing at the University of Arizona's sequencing core using a 3730 XL DNA analyser (Applied Biosystems, Inc.). Upon submitting the ITS sequence of this isolate to BLAST® (NCBI/NLM 2017), a >99% match was found with 19 strains of *Colletotrichum* sp. and 136 unidentified Neotropical endophytes (Supplementary Table S1). The ITS sequences from our isolate are available under GenBank accession numbers MG639894 and MG639895.

UV absorbance of secondary metabolites

The total absorbance of SM extracts across 220–350 nm was quantified using a photodiode array detector in-line with the UPLC-MS system. The 220–350 nm window was chosen based on inspection of raw data, which showed that *A. blackiana* and *B. utile* both had at least as much absorbance in UVA plus UVB as in UVC. Spectra within a bin size of 1 nm were summed and adjusted for the absorbance of a blank. This net absorbance was summed across the retention time associated with a given compound to yield the total absorbance for that compound.

Bioassays

We conducted two bioassays with SM extracts. The first, using a field-collected, pathogenic strain of fungus, assayed the inhibition of hyphal growth (Supplementary Fig. S2). Stock solutions of SMs were prepared at 7.5 mg ml^{-1} in 70:30 acetone:water (v/v). The fungus was prepared for the assay by first transferring hyphae from agar slants to 60 mm Petri plates with 4% (w/w) potato dextrose agar media, which were incubated at room temperature away from direct sunlight. Upon verifying the viability of the cultures in the Petri plates, hyphal plugs were transferred from Petri plates to 500 ml conical flasks filled to 300 ml with potato dextrose broth. Flasks were incubated at room temperature, without shaking, and away from direct sunlight. Once hyphae were visible in ~30% of the flask volume, the culture was homogenized for 30 s in a commercial blender and the assay was initiated. Immediately prior to adding the homogenized hyphae, the microplates were prepared with 75 µl of 4% (w/w) potato dextrose agar and the desired concentration of SM solution, which were combined while the agar was liquefied at ~60 °C to ensure thorough mixing. The mixture was then allowed to cool and the solvent allowed to evaporate inside a biosafety cabinet for 30 min, after which time 100 µl of culture broth was added to each well. All SM extracts were initially assayed at concentrations of 0, 0.5, 1.0, 2.5, and 5.0% mass of extract/mass of agar (w/w), and intermediate concentrations were assayed as necessary to establish growth inhibition curves. Each extract concentration was replicated in five wells. Each assay included five replicates of a positive control of nalidixic acid (500 mg ml^{-1} agar), a solvent control (50 µl of 70% acetone allowed to evaporate), a negative agar control to which culture broth was added (the 0% treatment), and a negative agar control to which no culture broth was added. Immediately after inoculation, the baseline absorbance at 700 nm was measured using a plate reader (Synergy H1, Biotek Instruments Inc.). Subsequent absorbance readings were taken at 24, 36, and 48 h, and the baseline was subtracted to calculate hyphal growth. During the assays, the plates were sealed with Parafilm® M (Bemis Company Inc., Oshkosh, WI, USA) and incubated at room temperature away from direct sunlight.

Once the assays were completed, we determined the SM dosage resulting in a 50% inhibition of hyphal growth (a unitless term, DW $extract_{GI50}$, calculated as mg of extract per 100 mg of agar) relative to a solvent (negative) control by fitting dose–response curves using the 'drc' package in R (Beckman, 2013; Ritz *et al.*, 2015). We multiplied $(DW\ extract_{GI50})^{-1}$ by DW $extract_{leaf}$, a unitless term calculated as the dry mass of SMs that was extracted per 100 mg dry mass of leaf (e.g. DW $extract_{leaf}$=30 mg for 30 mg of extract per 100 mg leaf DW). This accounted for the fact that leaves with more extract per DW should be more toxic. Hence, an inhibition index, *I*, was calculated using Equation 1:

$$I = \frac{[\text{DW extract}]_{\text{leaf}}}{[\text{DW extract}]_{\text{GI50}}} \quad (1)$$

For the second bioassay, we used the brine shrimp, *Artemia franciscana* Kellogg, as a model arthropod herbivore and assayed the lethality of SM extracts. *Artemia* have been used as bioassay organisms in ecotoxicology studies for decades, and more recently have proven useful in evaluating the toxicity of plant SMs (Beckman, 2013). We hatched *A. franciscana* from cysts (Brine Shrimp Direct, Ogden, UT, USA) according to the methods described by Beckman (2013). Stock solutions of SM extracts were prepared at 7.5 mg ml^{-1} in an aqueous solution of 3% aquarium salt (w/w, Milli-Q® water and Instant Ocean® salt, Spectrum Brands Inc., Blacksburg, VA, USA) and 2% DMSO (v/v) to dissolve intermediate polarity compounds. The *Artemia* assays were conducted in the same type of 96-well microplates as the fungal assays. To initiate each assay, 100 µl of 3% aquarium salt solution containing the desired concentration of SM extract was added to each well, followed by 100 µl of saltwater containing 20–60 *Artemia* larvae. Toxicity was scored as mortality. This was quantified visually at 24 h and 48 h using a dissecting scope and was expressed as the percentage of the original number of larvae added to each well that had subsequently experienced mortality. Glacial acetic acid diluted in 3% aquarium salt solution was used as a positive control at 0.01, 0.05, 0.1, and 0.5 µl ml^{-1}. Other controls included a solvent control (2% DMSO in saltwater, v/v) and a negative control (saltwater only). All extracts and controls were assayed in five replicates. SM extracts were assayed at 0.01, 0.05, and 0.5 mg ml^{-1} to begin to establish dose–response curves. However, extracts from both species began to precipitate at concentrations higher than 0.5 mg ml^{-1}, before a 50% reduction in survival was observed. As a result, lethality and statistical analyses were conducted using mortality values (% $mortality_{assay}$) for a single extract concentration of 0.05 mg ml^{-1} (DW $extract_{assay}$). As in the fungal assay, this was multiplied by DW $extract_{leaf}$. We calculated a lethality index, *L*, using Equation 2:

$$L = \frac{\%\ \text{mortality}_{\text{assay}}}{\%\ \text{mortality}_{\text{solvent\_control}}} \times \frac{[\text{DW extract}]_{\text{leaf}}}{[\text{DW extract}]_{\text{assay}}}$$

Results

Uniform shade treatments receive more PAR and UVB than sunfleck treatment

Although the USUV treatments received more PAR overall, SF treatment experienced higher maximum PPFD. Over the measurement period (31 August–17 September, 2014), the USUV treatments received 4.3-fold more total photosynthetic

photon flux per day as well as 66% higher midday (11.00–13.00 h) PPFD than did SF treatment (Supplementary Fig. S3). However, SF treatment received marginally (P=0.062) higher maximum PPFD than did the USUV treatments (63% higher averaged over the full measurement period and 71% higher averaged over the 15 d with cloudless periods).

The mean midday (11.00–13.00 h) UVB irradiances in the USUV treatments differed ~7.5-fold, with means ±SE of 763±19 mW m^{-2} in USUV+ and 102±2.5 mW m^{-2} in USUV–. Over the same period, SF treatment received no measurable UVB radiation. The irradiance in treatment USUV+ was ~11% of that measured in a large (>100 m^2) clearing. This is consistent with the UVB transmission rates of the plastic sheeting plus shade cloth, 11.2% and 1.5% (see the Materials and methods).

Total secondary metabolite content exhibits variable response to PAR and UVB

We used the dry weight of the extracted SMs per dry weight of leaf tissue as a metric of metabolic investment. For *A. blackiana*, the dry weight of SMs in mature leaves exhibited trends contrary to our expectations, showing either no change (USUV+) or a decline (USUV–) in response to higher PAR and UV as compared with treatment SF (Fig. 4). In contrast, results for mature leaves of *B. utile* were consistent with an expanded overall metabolic investment in SMs in response to increased PAR and UV, with both USUV treatments exhibiting higher SM weight than treatment SF (Fig. 4). In both species, SM weight in expanding leaves showed no response across treatments, consistent with physiological canalization during leaf expansion as seen in previous studies (Bixenmann *et al.*, 2011, 2016; Sinimbu *et al.*, 2012).

Up-regulation of phenolic compounds drives responses to increased PAR and UVB

Analysis via UPLC-MS and post-processing of data via XCMS (Smith *et al.*, 2006) yielded 101 putative compounds in *A. blackiana* and 286 in *B utile*, for all treatments and the two leaf ages combined (Fig. 1). Pairwise *t*-tests indicated differences in ion intensity for 29 compounds in *A. blackiana* and 129 compounds in *B. utile* in association with the experimental treatments. Further, both species exhibited induction as well as suppression of SMs across treatments, with *A. blackiana* inducing 16 and suppressing two in the USUV treatments relative to SF treatment and *B. utile* inducing 12 and suppressing 12 (Fig. 1). GNPS-linked database comparisons and molecular networking with MS/MS spectra resulted in class-level identification for 66% and 84% of the compounds in *A. blackiana* and *B. utile*, respectively (Fig. 1). Of these classifications, 100% (*A. blackiana*) and 88% (*B. utile*) were based on spectral library matches, and the remainder were based on nearest-neighbour matches in molecular networks. Phenolics were the most compound-rich class in both species, accounting for 48% of compounds in *A. blackiana* and 61% in *B. utile*.

In mature leaves of both species and expanding leaves of *B. utile*, phenolics, as expected, constituted the majority of compounds present at higher abundances in higher PAR and UV (Fig. 6). Moreover, each species' major classes of phenolics, HCAs in *A. blackiana* and HCAs as well as flavonoids in *B. utile*, all showed overall increases with PAR and UV that exceeded those of any other metabolite classes (Fig. 6). Phenolics also accounted for 87.5% of the compounds induced in mature leaves in higher PAR and UV in *A. blackiana* and 91.7% in *B. utile*, while accounting for only 0% and 25%, respectively, of compounds suppressed (Fig. 1). While unknown compounds showed significant increases in *B. utile*, this was due entirely to the overall increase in SM extract mass in the USUV treatments (Fig. 4), by which all fold changes were scaled during statistical analysis. Per milligram of SM extract, no individual unknown compounds increased and eight decreased in abundance in treatment USUV+ compared with treatment SF. Expanding leaves of *A. blackiana* exhibited minimal differences in SM abundances across treatments, with no induction or suppression of compounds, pointing to canalization as with overall SM extract weight.

Up-regulation of phenolic compounds and increased antioxidant power

Contrary to expectation, in neither species did we observe differences in the antioxidant power of primary metabolites with increasing PAR and UVB (Supplementary Table S4). This was the case for both expanding and mature leaves. However, the antioxidant power of SMs in mature leaves of both species followed our prediction, increasing with phenolic abundance in higher PAR and UVB (Figs 2, 6). This trend was evident in both species for the USUV+ treatment and in *B. utile* for the USUV– treatment, accounting for an increase in antioxidant power of >3-fold in each case. While in both species the

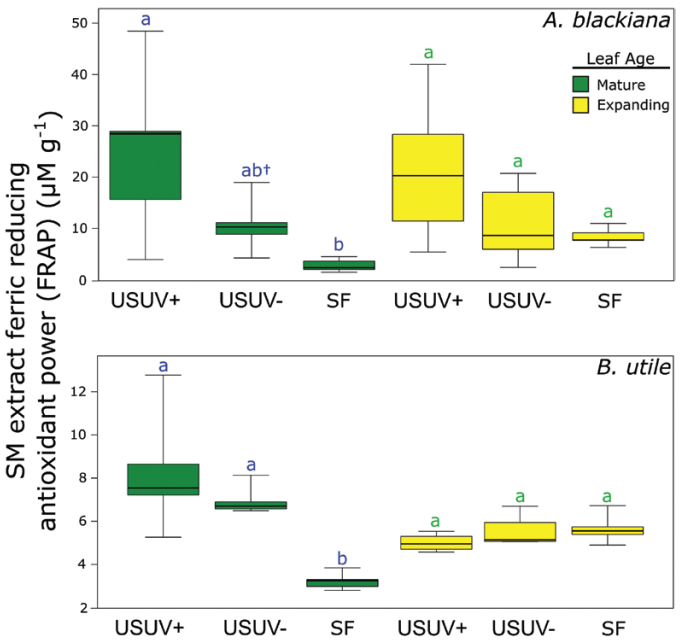

Fig. 2. Ferric reducing antioxidant power (FRAP) of secondary metabolite extracts. Antioxidant power is displayed as the ferric reducing equivalent of the secondary metabolite extract per gram of leaf tissue (DW). Pairwise statistical comparisons (Tukey's HSD) within leaf age resulting in $P \leq 0.05$ are indicated by non-matching letters above whiskers (n=5). Box and whisker specifications are per default boxplots in R statistical software. (This figure is available in colour at *JXB* online.)

antioxidant power of SMs showed an increase in the USUV+ treatment relative to the USUV– treatment, this trend was not statistically significant.

Up-regulation of phenolic compounds and increased UV absorbance

In mature leaves of both *A. blackiana* and *B. utile*, the total UV (220–350 nm) absorbance of SM extracts was generally higher in the USUV treatments than in the SF treatment, paralleling trends in phenolic abundance (Figs 3, 6). The exception to this trend was the USUV+ treatment of *B. utile*, in which high variance rendered the mean absorbance indistinguishable from those of USUV– treatment and SF treatment. In expanding leaves, *A. blackiana* exhibited no significant differences in absorbance across treatments, while in *B. utile* both of the USUV treatments exhibited higher absorbance than did SF treatment (Fig. 3). Finally, there were no differences in absorbance between SM extracts from the USUV+ and USUV– treatments regardless of leaf age.

Up-regulation of phenolic compounds and activity of secondary metabolite extracts against an invertebrate herbivore and a fungal pathogen

In the *Artemia* bioassay, the activity of SM extracts from *A. blackiana* did not differ across PAR and UVB treatments (Fig. 7). However, in both expanding and mature leaves of *B. utile*, SM extracts from treatment USUV+ induced higher *Artemia* mortality than did extracts from treatment SF (expanding. 44% higher mortality; mature, 129% higher mortality) (Fig. 7). Hence, in *B. utile*, peak *Artemia* mortality was associated with the peak of flavonoid phenolic abundance in the treatments with higher PAR and UVB (USUV+ and USUV–) (Fig. 6). This was the case for both expanding and mature leaves.

In the fungal assay, the SM extracts from *A. blackiana* demonstrating the strongest fungal growth inhibition were those from treatments SF (expanding leaves) and USUV– (Fig. 8). These trends in fungal growth inhibition across treatments did not parallel the overall shifts in abundance of any compound class, but rather were associated with the significant up-regulation of one compound in expanding leaves and of three compounds in mature leaves (Supplementary Table S3). One of these compounds was classified as a phenolic, while three were classified as phenol-based alkaloids (Supplementary Table S3). In contrast, the SM extracts from *B. utile* exhibited higher antifungal activity in both of the USUV treatments as compared with SF treatment (Fig. 8), paralleling the trends in activity and metabolite associations described for *B. utile* extracts in the *Artemia* assay. This was the case in both expanding and mature leaves.

Discussion: the evidence for multipurpose phenolics

While all chemical classes exhibited a combination of up-regulation and down-regulation among the constituent compounds, flavonoids and, to a lesser extent, HCA comprised the vast majority of compounds whose trends in abundance across treatments were associated with trends in abiotic as well

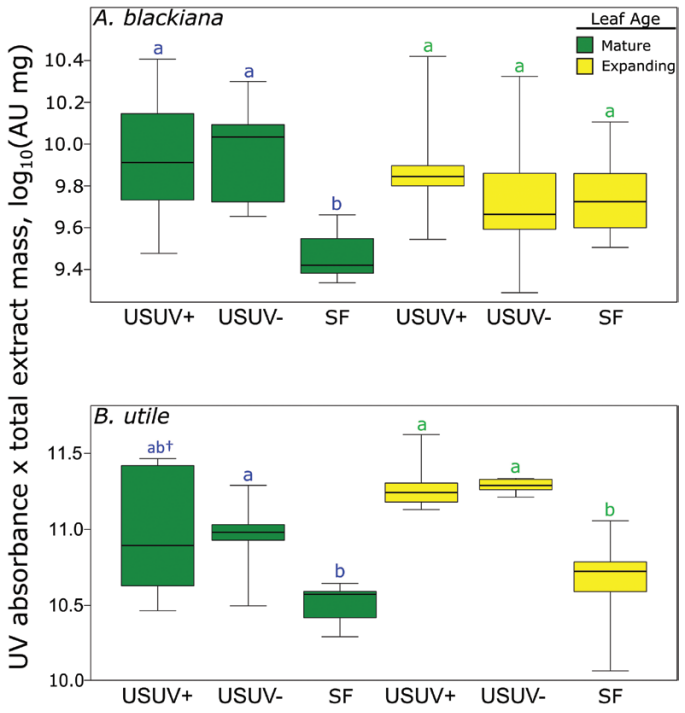

Fig. 3. UV (220–350 nm) absorbance of secondary metabolite extracts. Values are displayed as the $\log_{10}$-normalized absorbance of a standardized mass of secondary metabolite extract multiplied by the total mass of secondary metabolite extract per 100 mg of dried leaf material. Statistical comparisons are as in Fig. 2, with the addition of a dagger appended to the letters above a uniform shade treatment that exhibits marginal differences ($0.05<P\leq0.10$) from the sunfleck treatment (*A. blackiana*, $n=10$. *B. utile*, mature, $n=7$; expanding, $n=5$). (This figure is available in colour at *JXB* online.)

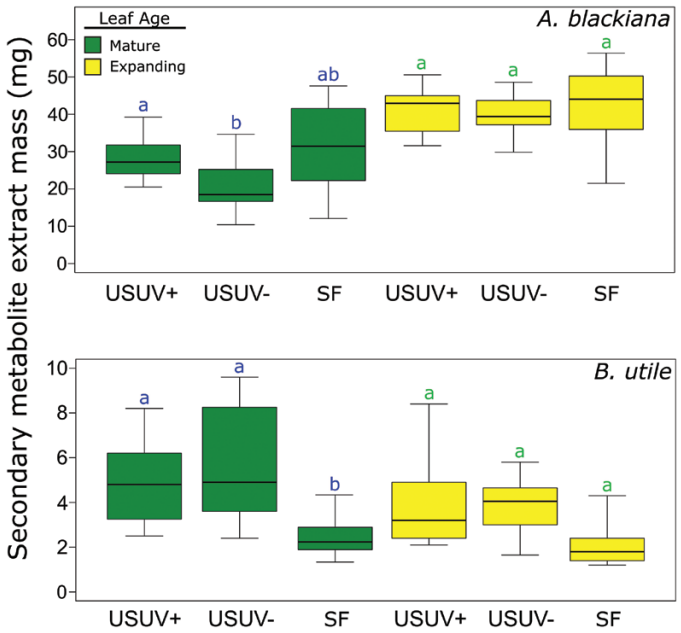

Fig. 4. Dry masses of secondary metabolite extracts per 100 mg of dried leaf material. Statistical comparisons are as in Fig. 3. (*A. blackiana*: mature, $n=16$; expanding, $n=13$. *B. utile*: mature, $n=7$; expanding, $n=5$). (This figure is available in colour at *JXB* online.)

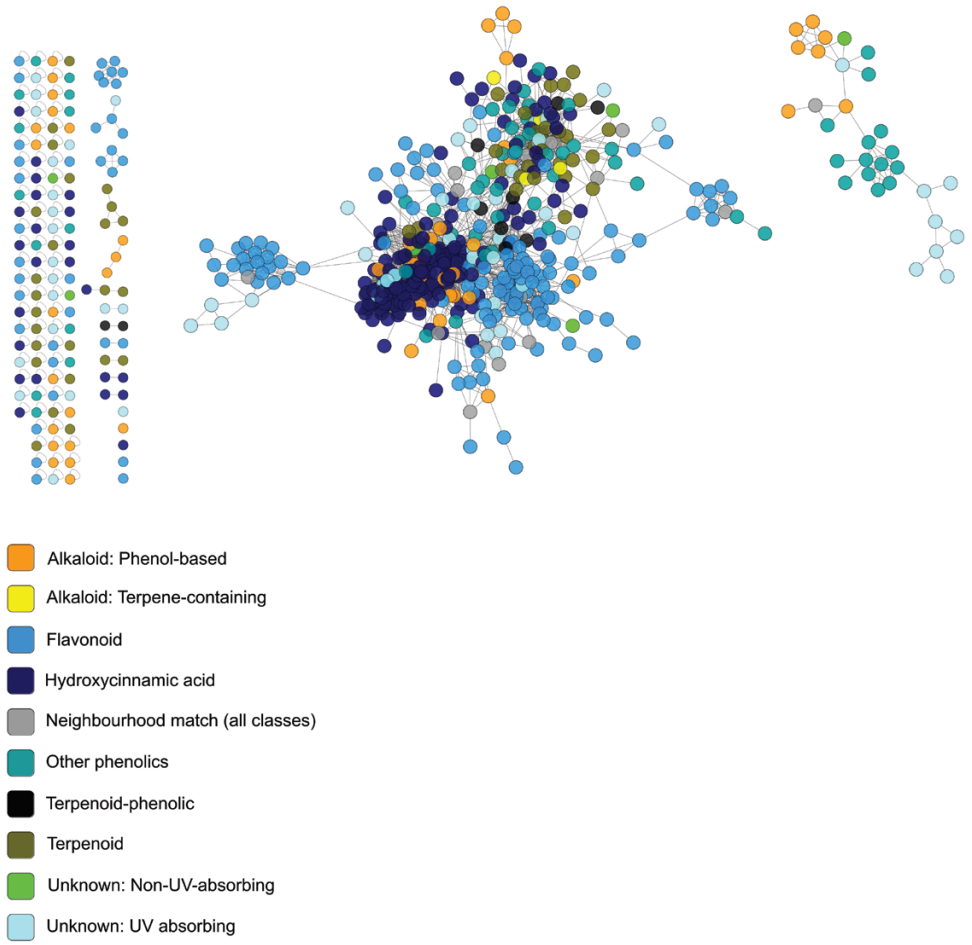

Fig. 5. Mass spectral molecular networks used for neighbourhood classification of secondary metabolites. The network shown is from *B. utile*. Each node is a metabolite, and connecting lines ('edges') indicate that two compounds are structurally related based on their MS/MS fingerprints. Unconnected nodes and groups of nodes indicate metabolites or groups of metabolites that are structurally unrelated to one another. For both expanding and mature leaves, networks were generated using five samples per treatment for *B. utile* and two samples per treatment for *A. blackiana*.

as biotic activity. In both *A. blackiana* and *B. utile*, the elevated abundances of these phenolics under increased UVB exposure and increased PAR were associated with increased levels of protection against abiotic stress, in the form of greater UV absorbance and antioxidant capacity (Figs 2, 3A reflected in the two bioassays (Figs 7, 8); these phenolics, particularly the flavonoids of *B. utile* (Fig. 6), were also associated with increased levels of biotic defence. Indeed, flavonoids and HCAs were the only classes of SMs that paralleled the trends of toxicity across treatments, with alkaloids, terpenoids, and even other classes of phenolics exhibiting weak or variable trends in contrast (Fig. 6). These trends, in turn, are consistent with dual abiotic and biotic functions of particular phenolics, probably playing a part in allowing shade-tolerant tropical trees to acclimate to concurrent increases in solar radiation and pest pressure in a metabolically efficient manner.

Role of phenolics in protection against abiotic stress

The contribution of HCAs to the UV absorbance of SM extracts is most evident in the case of mature leaves of *A. blackiana*. Here, HCAs were the only class of SMs whose shifts in abundance paralleled the increases in UV absorbance (Figs 2, 3, 6). This was evident across both levels of increased UV exposure; that is, from treatment SF to USUV– and from USUV– to USUV+.

In *B. utile*, the contribution of HCAs to the UV absorbance of SM extracts cannot be isolated in all cases from that of flavonoids. However, it is clear that HCAs, flavonoids, or a combination of the two contributed to increases in UV absorbance in the USUV treatments in both expanding and mature leaves (Figs 1, 2).

Our results are in line with the known structural properties of HCAs and flavonoids. Both structural classes have absorption peaks in or near the UVB and both are recognized as protecting plants against UV (Landry *et al.*, 1995; Burchard *et al.*, 2000, Ryan *et al.*, 2001). The molar extinction coefficients range from 20 000 M^{-1} cm^{-1} to 25 000 M^{-1} cm^{-1} for flavonoids and from 15 000 M^{-1} cm^{-1} to 20 000 M^{-1} cm^{-1} for HCAs (Chen and Ahn, 1998). Using the red peak of Chl *a*, at ~78 000 M^{-1} cm^{-1}, as a benchmark for very effective absorption, it is clear that both flavonoids and HCAs efficiently absorb UVB.

In both *A. blackiana* and *B. utile*, increases in the antioxidant power of the SM extracts (Fig. 2) were consistent with the proposed function of flavonoids and/or HCAs in contributing to the maintenance of the redox state of plant cells

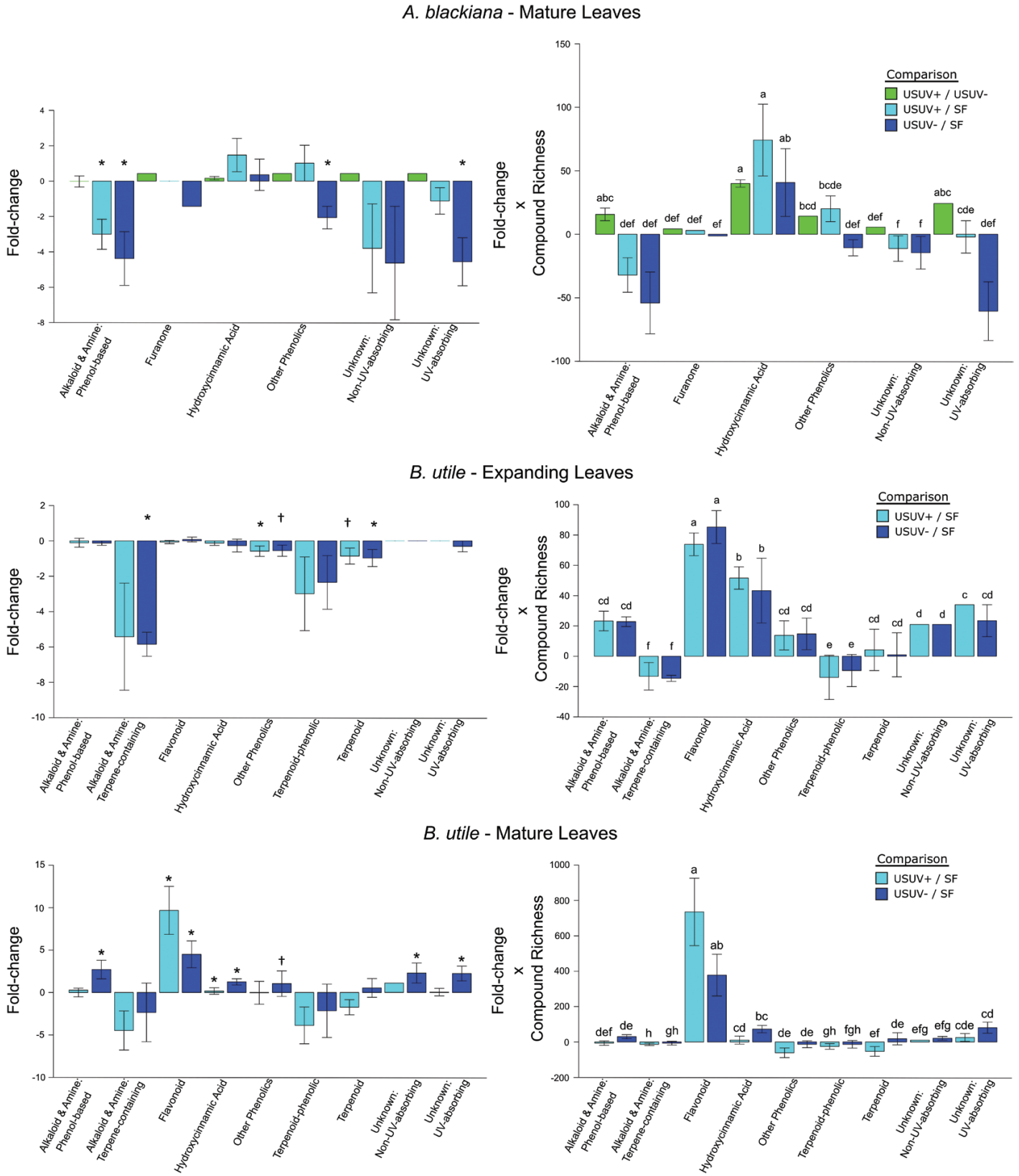

Fig. 6. Mean abundance shifts of secondary metabolite types. Daggers indicate differences between the uniform shade treatments versus the sunfleck treatment at $P \leq 0.05$ for the metabolite type to which they are appended (*A. blackiana*, mature, $n=8$; expanding, $n=10$; *B. utile*, mature, $n=7$; expanding, $n=5$). (This figure is available in colour at *JXB* online.)

(Agati *et al.*, 2013). It is important to note that, while both flavonoids and HCAs were associated with increased antioxidant power, these results must be interpreted cautiously. As first proposed by Takahama (1992), for phenolics to be effective antioxidants, the oxidized phenolics, phenoxyl radicals, must be regenerated to their reduced forms. Although

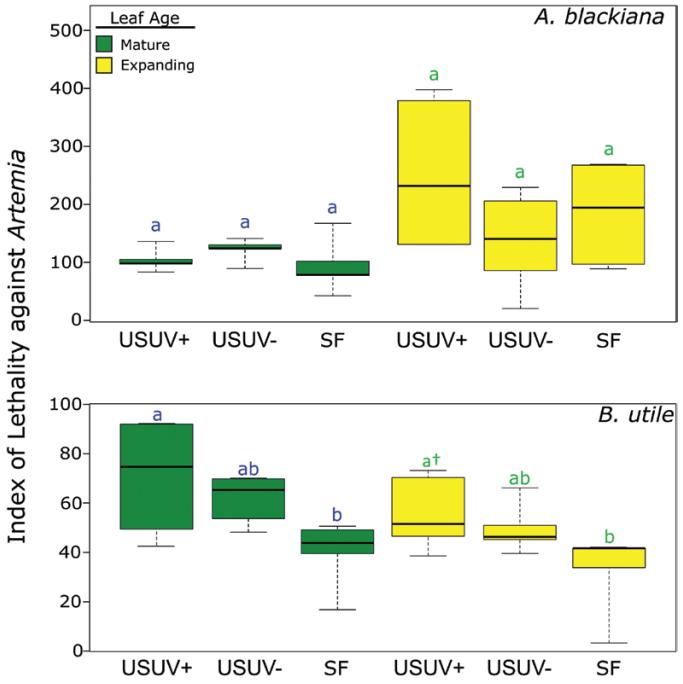

Fig. 7. Lethality index of secondary metabolite extracts against *Artemia* shrimp. Higher values on the *y*-axis indicate increasing lethality. *n*=5. Statistical comparisons are as in Fig. 3. (This figure is available in colour at *JXB* online.)

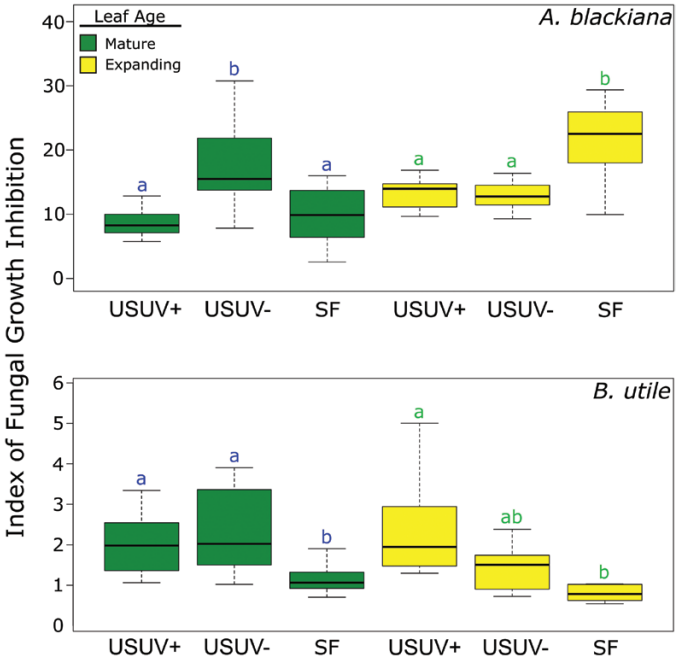

Fig. 8. Inhibition index of secondary metabolite extracts against fungus hyphal growth. Higher values on the *y*-axis indicate increasing inhibition (*A. blackiana*. mature, *n*=14; expanding, *n*=12; *B. utile*, mature, *n*=7; expanding, *n*=5). Statistical comparisons are as in Fig. 3. (This figure is available in colour at *JXB* online.)

some evidence indicates that such mechanisms exist, particularly in the vacuole where ascorbic acid may regenerate the parent phenolics (Takahama and Oniki, 1997; Ferreres *et al.*, 2011), more support for biochemical cycles that regenerate parent phenolics is necessary in order to demonstrate that phenolics are effective antioxidants *in planta* (Grace and Logan, 2000).

Biotic defence role of phenolics

In addition to regulatory trends consistent with roles in protection against abiotic stress, increases in the flavonoids and HCAs of *B. utile* were associated with increased activity of the SM extract against both an invertebrate herbivore (Fig. 7) and a fungal pathogen (Fig. 8). The concomitant decreases of alkaloids and terpenoids amid the increases in flavonoids and HCAs in mature leaves allow us to assign this biotic activity to the latter with some certainty. This is consistent with the hypothesized activity of these phenolics as deterrents of herbivores and pathogens.

HCAs did not show strong associations with biotic activity in our assays of *A. blackiana* SMs, and this may be due to our use of non-specialized bioassay organisms. In further testing, efforts should be made to assay the activity of *A. blackiana* SMs using the pests with which it interacts *in situ*.

Phenolics comprise multiple functional roles

Overall, our metabolomic data and assays suggest that the phenolics employed by each species in the transition from sunflecks to environments with higher PAR, UVB, and pest pressure may be endowed with multiple functional roles. While these trends were clear at the class level for flavonoids and, to some extent, for HCAs, the finer scale of metabolomics data allowed us to capture the small subset of phenolics that were associated with antifungal activity in *A. blackiana*. Upon comparing assayed activity trends with shifts in abundance of individual compounds, a picture emerged of flavonoids and HCAs as comprising compounds with the potential for multiple simultaneous roles *in planta*.

Shade-tolerant tropical trees such as *A. blackiana* and *B. utile* have evolved in habitats with periodic, concurrent increases in PAR availability, UV light exposure, and pest pressure due to gap formation and canopy thinning by falling branches or trees. For such species, we hypothesized that up-regulated phenolics derived from the additional photosynthate via increased PAR may be employed to mitigate the accompanying abiotic and biotic stressors. Our results bear out this hypothesis. In this study, although we only examined the shaded end of the light gradient, we saw considerable increases in carbon allocation to phenolics with increasing PAR availability. Given the phylogenetically widespread capacity of angiosperms to divert surplus photosynthate to the shikimic acid pathway (Koricheva *et al.*, 1998; Maeda and Dudareva, 2012), through which phenolics are produced, this pathway may be ideally suited for phenotypic plasticity in response to shifts in the light environment. Given that phenolics exhibit considerable structural diversity (>8000 described; Harborne, 1993), those phenolics with the structural elements that contribute to UV absorbance and antioxidant power as well as anti-herbivore/anti-pathogen activity may be ideally suited to respond simultaneously to biotic and abiotic stressors when they act in parallel, such as for shade-tolerant plants in patches of decreased canopy cover. Thus, our study demonstrates the insights into the chemical

ecology and ecophysiology of shade-tolerant tropical trees to be gained when metabolomic analyses, including the identification of specific compound classes, combined with bioassays, allow the multiple functional capabilities of phenolics to be taken into account.

Supplementary data

Supplementary data are available at *JXB* online.

Table S1. BLAST® ITS sequence matches for the field-collected fungal pathogen.

Table S2. Leaf angle comparison.

Table S3. Secondary metabolites associated with fungal inhibition.

Fig. S1. Photos of experimental conditions.

Fig. S2. Photos of bioassay conditions.

Fig. S3. PAR levels in treatments.

Fig. S4. Chromatograms and photodiode array traces for samples from all treatments representing each species and leaf age.

Acknowledgements

We would like to dedicate this work to our co-author and dear colleague Thomas Kursar, who sadly passed away before publication. We are grateful to the following individuals and organizations for assistance with and support for this project. Mariana Franco, Steven Pappas, Justin Shaffer, and Kayla Garcia provided assistance in the field and the laboratory. Oris Acevedo, Raineldo Urriola, Argelis Ruiz, and Klaus Winter assisted with logistics in Panama. A. Elizabeth Arnold provided facilities and valuable input for the fungal bioassays. Susan Whitehead, Nick Smirnoff, and two anonymous reviewers provided valuable comments on the manuscript. Computing was greatly facilitated by the Center for High Performance Computing at the University of Utah, and by the Open Science Grid, which is supported by U.S. NSF award 1148698, and the U.S. DOE Office of Science. The environment ministry of Panama granted collecting and export permits (SE/P-15-13, SE/P-11-14). The U.S. National Science Foundation funded GFS (DEB-1405637) and Dimensions of Biodiversity to TAK and PDC (DEB-1135733). GFS was also funded by the U.S. Environmental Protection Agency (F13F31245).

Data deposition

Ferric reducing antioxidant power (FRAP) data collected from both species and leaf ages and all treatments; *Artemia* bioassay data collected from both species and leaf ages and all treatments; fungal pathogen bioassay data collected from both species and leaf ages and all treatments; UV absorbance of secondary metabolite extracts collected from both species and leaf ages and all treatments; gravimetric data for secondary metabolite extracts collected from both species and leaf ages and all treatments; PAR, UV, and meteorological data collected from all experimental treatments; R code for processing and analysis of UPLC-MS data with XCMS and MetaboAnalyst; detailed results of statistical analyses of secondary metabolite fold change across treatments for both species and leaf ages and all treatments; classification and fold change data for each compound across both species and leaf ages and all treatments; molecular network visualization files for both species. Dryad Digital Repository. https://doi.org/10.5061/dryad.t469v60.

Raw UPLC-MS and UPLC-MS/MS data files from both species and leaf ages and all treatments. MetaboLights (Haug *et al.*, 2013). https://www.ebi.ac.uk/metabolights/MTBLS1030.

References

Agati G, Tattini M. 2010. Multiple functional roles of flavonoids in photoprotection. New Phytologist **186**, 786–793.

Agati G, Brunetti C, Di Ferdinando M, Ferrini F, Pollastri S, Tattini M. 2013. Functional roles of flavonoids in photoprotection: new evidence, lessons from the past. Plant Physiology and Biochemistry **72**, 35–45.

Agrios GN. 2005. Plant pathology. Burlington, MA: Elsevier Academic Press.

Allen F. 2016. Trained models for ESI-MSMS. https://sourceforge.net/p/cfm-id/code/HEAD/tree/supplementary_material/trained_models/esi_msms_models/. Accessed 13 March 2019.

Allen F, Greiner R, Wishart D. 2014. Competitive fragmentation modeling of ESI-MS/MS spectra for putative metabolite identification. Metabolomics **11**, 98–110.

Arbona V, Manzi M, Ollas Cd, Gómez-Cadenas A. 2013. Metabolomics as a tool to investigate abiotic stress tolerance in plants. International Journal of Molecular Sciences **14**, 4885–4911.

Barber NA, Marquis RJ. 2011. Light environment and the impacts of foliage quality on herbivorous insect attack and bird predation. Oecologia **166**, 401–409.

Beckman NG. 2013. The distribution of fruit and seed toxicity during development for eleven neotropical trees and vines in Central Panama. PLoS One **8**, e66764.

Bennett RN, Wallsgrove RM. 1994. Secondary metabolites in plant defence mechanisms. New Phytologist **127**, 617–633.

Benzie IF, Strain JJ. 1999. Ferric reducing/antioxidant power assay: direct measure of total antioxidant activity of biological fluids and modified version for simultaneous measurement of total antioxidant power and ascorbic acid concentration. Methods in Enzymology **299**, 15–27.

Bixenmann RJ, Coley PD, Kursar TA. 2011. Is extrafloral nectar production induced by herbivores or ants in a tropical facultative ant–plant mutualism? Oecologia **165**, 417–425.

Bixenmann RJ, Coley PD, Weinhold A, Kursar TA. 2016. High herbivore pressure favors constitutive over induced defense. Ecology and Evolution **6**, 6037–6049.

Burchard P, Bilger W, Weissenböck G. 2000. Contribution of hydroxycinnamates and flavonoids to, epidermal shielding of UV-A and UV-B radiation in developing rye primary leaves as assessed by ultraviolet-induced chlorophyll fluorescence measurements. Plant, Cell & Environment **23**, 1373–1380.

Chazdon R, Pearcy R, Lee D, Fetcher N. 1996. Photosynthetic responses of tropical forest plants to contrasting light environments. In: Mulkey SS, Chazdon RL, Smith AP, eds. Tropical forest plant ecophysiology. New York: Chapman and Hall, 5–55.

Chen X, Ahn DU. 1998. Antioxidant activities of six natural phenolics against lipid oxidation induced by Fe^{2+} or ultraviolet light. Journal of the American Oil Chemists' Society **75**, 1717–1721.

Coley P, Barone J. 1996. Herbivory and plant defenses in tropical forests. Annual Review of Ecology and Systematics **27**, 305–335.

Dalling JW, Winter K, Andersen KM, Turner BL. 2013. Artefacts of the pot environment on soil nutrient availability: implications for the interpretation of ecological studies. Plant Ecology **214**, 329–338.

da Silva RR, Wang M, Nothias LF, van der Hooft JJJ, Caraballo-Rodríguez AM, Fox E, Balunas MJ, Klassen JL, Lopes NP, Dorrestein PC. 2018. Propagating annotations of molecular networks using in silico fragmentation. PLoS Computational Biology **14**, e1006089.

Endara MJ, Weinhold A, Cox JE, Wiggins NL, Coley PD, Kursar TA. 2015. Divergent evolution in antiherbivore defences within species complexes at a single Amazonian site. Journal of Ecology **103**, 1107–1118.

Ferreres F, Figueiredo R, Bettencourt S, *et al*. 2011. Identification of phenolic compounds in isolated vacuoles of the medicinal plant *Catharanthus roseus* and their interaction with vacuolar class III peroxidase: an H_2O_2 affair? Journal of Experimental Botany **62**, 2841–2854.

Flint S, Caldwell M. 1998. Solar UV-B and visible radiation in tropical forest gaps: measurements partitioning direct and diffuse radiation. Global Change Biology **4**, 863–870.

Grace SC, Logan BA. 2000. Energy dissipation and radical scavenging by the plant phenylpropanoid pathway. Philosophical Transactions of the Royal Society B: Biological Sciences **355**, 1499–1510.

Grayer RJ, Harborne JB. 1994. A survey of antifungal compounds from higher plants, 1982–1993. Phytochemistry **37**, 19–42.

Gu J, Gui Y, Chen L, Yuan G, Lu HZ, Xu X. 2013. Use of natural products as chemical library for drug discovery and network pharmacology. PLoS One **8**, e62839.

Harborne JB. 1993. The flavonoids—advances in research since 1986. London: Chapman and Hall.

Haug K, Salek RM, Conesa P, *et al*. 2013. MetaboLights—an open-access general-purpose repository for metabolomics studies and associated meta-data. Nucleic Acids Research **41**, D781–D786.

Jansen JJ, Allwood JW, Marsden-Edwards E, van der Putten WH, Goodacre R, van Dam NM. 2009. Metabolomic analysis of the interaction between plants and herbivores. Metabolomics **5**, 150–161.

Jansen MA, Gaba V, Greenberg BM. 1998. Higher plants and UV-B radiation: balancing damage, repair and acclimation. Trends in Plant Science **3**, 131–135.

Kolb CA, Käser MA, Kopecký J, Zotz G, Riederer M, Pfündel EE. 2001. Effects of natural intensities of visible and ultraviolet radiation on epidermal ultraviolet screening and photosynthesis in grape leaves. Plant Physiology **127**, 863–875.

Koricheva J, Larsson S, Haukioja E, Keinänen M, Keinanen M. 1998. Regulation of woody plant secondary metabolism by resource availability: hypothesis testing by means of meta-analysis. Oikos **83**, 212–226.

Kuhl C, Tautenhahn R, Böttcher C, Larson TR, Neumann S. 2012. CAMERA: an integrated strategy for compound spectra extraction and annotation of liquid chromatography/mass spectrometry data sets. Analytical Chemistry **84**, 283–289.

Landry LG, Chapple CC, Last RL. 1995. Arabidopsis mutants lacking phenolic sunscreens exhibit enhanced ultraviolet-B injury and oxidative damage. Plant Physiology **109**, 1159–1166.

Levin DA. 1971. Plant phenolics: An ecological perspective. The American Naturalist **105**, 157–181.

Maeda H, Dudareva N. 2012. The shikimate pathway and aromatic amino acid biosynthesis in plants. Annual Review of Plant Biology **63**, 73–105.

Pordes R, Petravick D, Kramer B, *et al*. 2007. The open science grid. Journal of Physics: Conference Series **78**, 012057.

Richards LA, Coley PD. 2007. Seasonal and habitat differences affect the impact of food and predation on herbivores: a comparison between gaps and understory of a tropical forest. Oikos **116**, 31–40.

Ritz C, Baty F, Streibig JC, Gerhard D. 2015. Dose–response analysis using R. PLoS One **10**, e0146021.

Ryan KG, Swinny EE, Winefield C, Markham KR. 2001. Flavonoids and UV photoprotection in Arabidopsis mutants. Zeitschrift fur Naturforschung C **56**, 745–754.

Salgado-Luarte C, Gianoli E. 2010. Herbivory on temperate rainforest seedlings in sun and shade: resistance, tolerance and habitat distribution. PLoS One **5**, e11460.

Schneider GF, Coley PD, Younkin GC, Forrister DL, Mills AG, Kursar TA. 2019. Data from: Phenolics lie at the center of functional versatility in the responses of two phytochemically diverse tropical trees to canopy thinning. Dryad Digital Repository. https://doi.org/10.5061/dryad.t469v60.

Sedio BE, Rojas Echeverri JC, Boya P CA, Wright SJ. 2017. Sources of variation in foliar secondary chemistry in a tropical forest tree community. Ecology **98**, 616–623.

Sfiligoi I, Bradley DC, Holzman B, Mhashilkar P, Padhi S, Wurthwein F. 2009. The pilot way to Grid resources using glideinWMS. WRI World Congress on Computer Science and Information Engineering **2**, 428–432.

Shannon P, Markiel A, Ozier O, Baliga NS, Wang JT, Ramage D, Amin N, Schwikowski B, Ideker T. 2003. Cytoscape: a software environment for integrated models of biomolecular interaction networks. Genome Research **13**, 2498–2504.

Sinimbu G, Coley PD, Lemes MR, Lokvam J, Kursar TA. 2012. Do the antiherbivore traits of expanding leaves in the Neotropical tree *Inga paraensis* (Fabaceae) vary with light availability? Oecologia **170**, 669–676.

Smith CA, Want EJ, O'Maille G, Abagyan R, Siuzdak G. 2006. XCMS: processing mass spectrometry data for metabolite profiling using nonlinear peak alignment, matching, and identification. Analytical Chemistry **78**, 779–787.

Takahama U. 1992. Hydrogen peroxide scavenging systems in vacuoles of mesophyll cells of *Vicia faba*. Phytochemistry **31**, 1127–1133.

Takahama U, Oniki T. 1997. A peroxidase/phenolics/ascorbate system can scavenge hydrogen peroxide in plants cells. Physiologia Plantarum **101**, 845–852.

Wang M, Carver JJ, Phelan VV, *et al*. 2016. Sharing and community curation of mass spectrometry data with Global Natural Products Social Molecular Networking. Nature Biotechnology **34**, 828–837.

Wiggins NL, Forrister DL, Endara MJ, Coley PD, Kursar TA. 2016. Quantitative and qualitative shifts in defensive metabolites define chemical defense investment during leaf development in *Inga*, a genus of tropical trees. Ecology and Evolution **6**, 478–492.